European Journal of Radiology Open 10 (2023) 100464

Contents lists available at ScienceDirect

European Journal of Radiology Open

journal homepage: www.elsevier.com/locate/ejro

Preoperative evaluation of malignant pancreatobiliary obstruction: A novel technique for multiphase fusion 3D CT images

Bin Li, FengQi Lu, JianMing Ni, WenJuan Wu, HuiTing Xu, ZhuiYang Zhang *

Department of Radiology, The Affiliated Wuxi No.2 People's Hospital of Nanjing Medical University, 68 Zhongshan Rd., Jiangsu 214002, PR China

ARTICLE INFO

Keywords:
CT
CT angiography
Negative-contrast CT cholangiopancreatography
Multiphase fusion images
3D
Malignant pancreatobiliary obstruction

ABSTRACT

The purpose of this article is to describe a novel technique of multiphase fusion three-dimensional (3D) images in patients with malignant pancreatobiliary obstruction. Multiphase fusion 3D images of CT arteriography, portovenography and hepatic venography combined with negative-contrast CT cholangiopancreatography can be done with enhanced multiphase CT scan using intravenous contrast agent at once. This technique may be feasible for one-stop evaluation of malignant pancreatobiliary obstruction.

1. Introduction

Although malignant pancreatobiliary obstruction usually caused by a variety of local malignancy, such as cholangiocarcinoma, pancreatic carcinoma, hepatocellular carcinoma, ampullary carcinoma, gallbladder carcinoma, or metastasis to the regional lymph nodes [1], clinical strategies for the management of these disorders differ including the need for- and type of surgery [2]. In order to improve curative rates, precise staging and knowledge of the regional anatomy between tumor and surrounding structures are essential. Therefore, preoperative imaging evaluation concerning a suspected malignant obstruction traditionally requires multimodality imaging for the purpose of correct and complete diagnosis, such as ultrasound, computed tomography (CT), magnetic resonance imaging (MRI), or even invasive procedures of endoscopic retrograde cholangiopancreatography (ERCP), percutaneous transhepatic cholangiography (PTC), or both. Thus, high cost and longer work-up time for patients are inevitable [3]. Recent developments in multidetector CT (MDCT) technology provide rapidly acquired multiphase datasets during each phase of maximum vascular and parenchymal enhancement using sub-millimeter section, and allowing reconstruction of three-dimensional (3D) CT angiography and negative-contrast CT cholangiopancreatography (nCTCP) images [4]. Meanwhile, multiphase 3D CT angiography/CT cholangiography image fusion can be generated by means of a dedicated workstation [5]. In view of this, one-stop evaluation of the regional anatomy between tumor and adjacent structures are desirable for surgeons [6]. In this article, we describe a novel method for multiphase fusion imaging in 13 male and 17 female patients (mean age, 62 years; range, 49–82 years) without distant metastases who underwent curative or palliative treatment with malignant pancreatobiliary obstruction.

2. Imaging technique

All CT scans were performed with a 320-MDCT scanner (Aquilion one, Toshiba Medical Systems). Patients were routinely instructed to fast for 8–10 h prior to the CT examination and each patient was asked to drink 500–800 ml of water 30 min before scanning to distend the gastrointestinal tract. The standard scanning protocol in our hospital mainly consists of unenhanced and biphasic contrast enhanced scans in a single breath-hold (4–5 s) for each of the sequence. An automatic trigger scanning mode with a 10 s delay was used when a region of interest was set on the descending aorta, of which the preset CT number was 200 Hounsfield units. For this mode, the arterial and portal venous phase were a delay of 35–42 s and 65–78 s, respectively, after starting the injection of 90–100 ml of nonionic contrast agent (Optiray 320, Tyco Healthcare, Quebec, Canada) at a rate of 3–4 ml/s through the antecubital vein. The parameters were at 120 kVp; 0.5 s scanning time per rotation; detector collimation of 0.5 mm × 64 with a pitch factor of

* Corresponding author.
E-mail addresses: libin3189@163.com (B. Li), lufqi@163.com (F. Lu), jianming_ni@me.com (J. Ni), happybobo82@163.com (W. Wu), 914484179@qq.com (H. Xu), zhangzhuiyang@163.com (Z. Zhang).

https://doi.org/10.1016/j.ejro.2022.100464
Received 16 June 2022; Accepted 7 December 2022

0.828; tube current with automatic dose modulation ranging from 97 to 307 mA; field of view (FOV) of 30–34 cm.

For the arterial and portal venous phase raw data, their volume data were automatically reconstructed with the slice thickness of 1.0 mm and reconstruction interval of 1.0 mm, same FOV as above. Then, the portal venous phase raw data was reconstructed once again for nCTCP with a low spatial resolution algorithm for reducing the image noise [7,8], and other parameters included: the slice thickness of 0.5 mm; reconstruction interval of 0.5–1.0 mm; matrix of 512 × 512; FOV of 22–34 cm. All reconstructed axial source images (volume data) were transferred to a workstation (Advantage Workstations, version 4.6, GE Medical Systems) for further image postprocessing.

3. Image postprocessing

3.1. CT arteriography

Because of 3D CT arteriography (CTAG) is as accurate as digital subtraction angiography for the assessment of hepatobiliary arterial anatomy [5], arterial evaluation can be concisely depicted with the late arterial phase in either maximum intensity projection (MIP) or volume rendering (VR) mode. In patients with malignant pancreatobiliary obstruction, preoperative knowledge of the blood supply of tumor derived from main hepatic and peripancreatic arteries (Fig. 1), arterial tumor contact (Fig. 2), or arterial variants, such as replaced or accessory right or left hepatic artery (Figs. 3 and 4) is crucial to surgery planning [7–10].

3.2. CT portovenography and hepatic venography

In the absence of distant metastasis, the most important veins that can affect tumor resectability include the portal vein and superior mesenteric vein [9]. CT portovenography (CTPV) is helpful to evaluate the morphology and relationship of these veins with the surrounding structures, the degree of tumor invasion, and whether or not collaterals presented in patients with abdominal malignancies (Figs. 2–4). On the other hand, CT hepatic venography (CTHV) may aid surgical planning because it helps surgeons selected hepatectomy of either the right or left lobe of the liver [5]. However, the portal vein and hepatic vein were often opacified concomitantly during the portal phase, thought the enhancement of them might be different in this study. To extract the portal vein and hepatic vein respectively, we used one of segment tools for small vessels on the workstation, which has the function to automatically add or remove object vessels depended on each vascular anatomy.

3.3. Negative-contrast CT cholangiopancreatography

Different from previous reports [5, 6, 8], a subvolume 3D nCTCP with MinIP were generated using the volume data during the portal venous phase with 3D tools according to the published literatures [4, 11]. The imaging principle is based on the dilated bile ducts as a negative contrast agent for differentiation from the surrounding enhanced hepatic and pancreatic parenchyma without additional biliary contrast agent [12]. This technique was useful for identifying obstructive level, depicting complex biliary tree anatomy, and providing entire

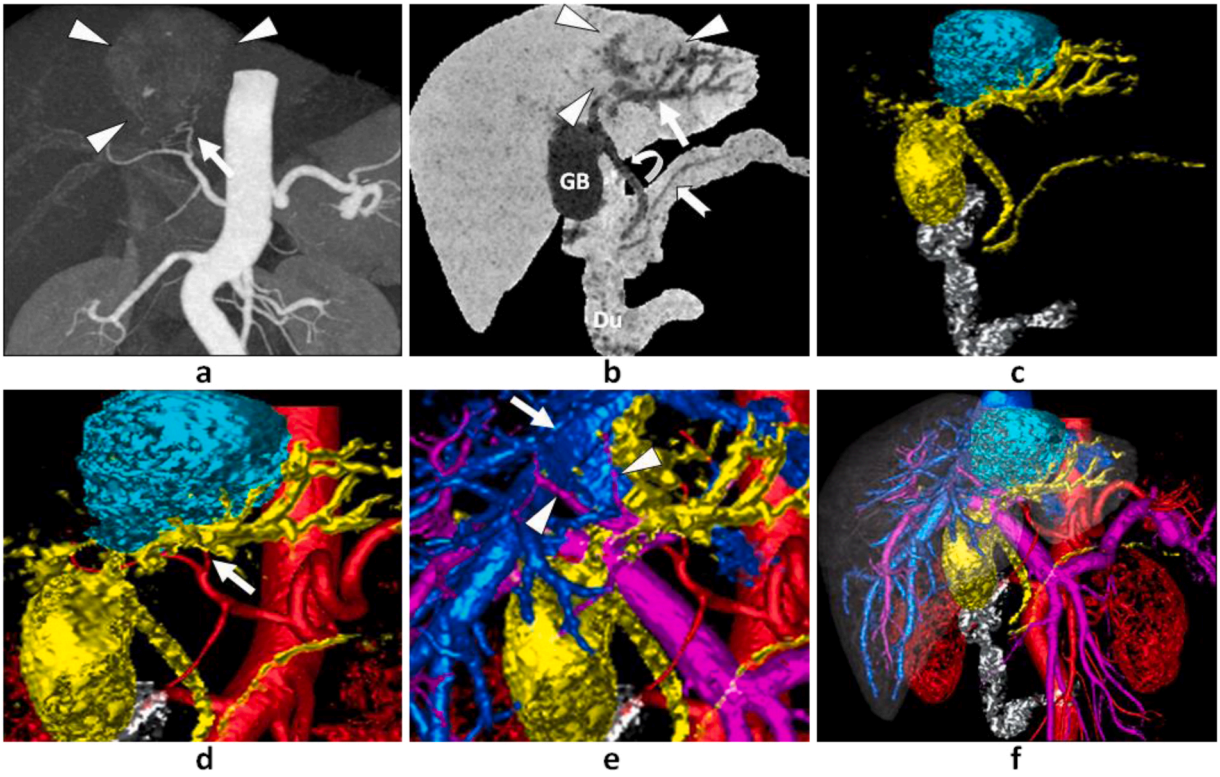

Fig. 1. A 61-year-old woman with hepatocellular carcinoma in the left hepatic lobe underwent curative treatment of left hemihepatectomy. On 3D CTAG with MIP (a), an enhanced tumor (arrowheads) in the left hepatic lobe during the late arterial phase whose blood supply derived from the left hepatic artery (arrow) is noted. On 3D nCTCP with MinIP (b), it demonstrates a relative hypodense tumor (arrowheads) during the portal venous phase with dilated left intrahepatic ducts caused by the tumor (arrow) and normal extrahepatic duct (curved arrow) and pancreatic duct (tailed arrow). Multiphase fusion 3D images with VR, which consisted of different observed structures according to the clinical needs can be showed (c-f), such as 3D nCTCP (yellow) with the duodenal (gray) distinctly depicting the spatial relationship between the tumor (green) and dilated left intrahepatic ducts (c) or blood supply of the tumor that originated from the left hepatic artery (arrow, d); delineating the depressed middle hepatic vein (arrow, blue) and left portal vein branches (arrowheads, purple) (e) caused by the tumor, or entirely depicting spatial relations of the tumor in the liver (25 % of transparency) to intrahepatic ducts and hepatic vessels (f). GB, gallbladder; Du, duodenum. (For interpretation of the references to color in this figure legend, the reader is referred to the web version of this article.)

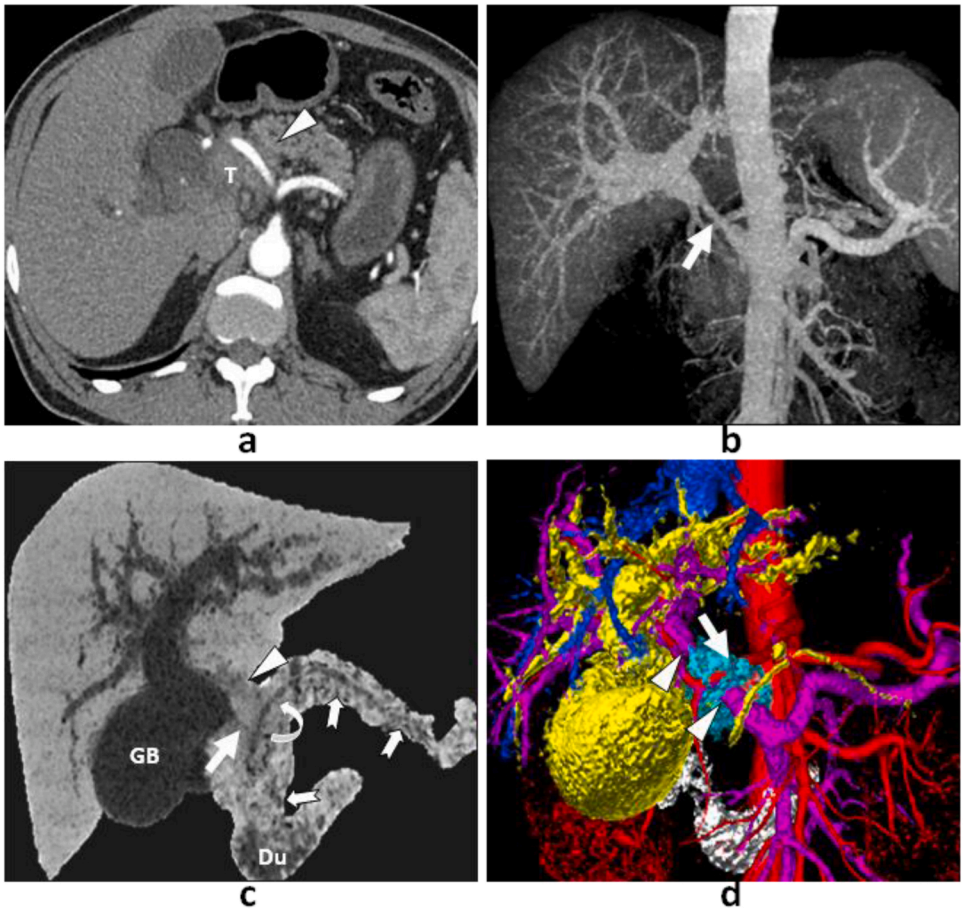

Fig. 2. A 51-year-old man with extrahepatic ductal carcinoma underwent palliative treatment of intraoperatively external biliary drainage. CTAG (a) demonstrates tumor (T) encasement of the common hepatic artery (arrowhead) as well as narrowing of the main portal vein (arrow) on 3D CTPV with MIP (b), which suggests tumor vessel invasion. 3D nCTCP with MinIP (c) shows abrupt narrowing of the common bile duct at suprapancreatic segment (arrow) with a hypodense tumor (arrowhead) also at this location. Pancreatic fatty infiltration, which demonstrates as patches of hypodense pattern (tailed arrows) is noted; however, nondilated pancreatic duct is discernible (curved arrow). Multiphase fusion 3D images with VR (d) consisted of the pancreatobiliary system (yellow), duodenum (gray), tumor (green), main peripancreatic arteries (red), portal vein (purple), and hepatic vein (blue) depict tumor encasement of the common hepatic artery (arrow) and portal vein (arrowheads), which suggest unresectable tumor. GB, gallbladder; Du, duodenum. (For interpretation of the references to color in this figure legend, the reader is referred to the web version of this article.)

pancreatobiliary system in one image similar to of 3D MR cholangiopancreatography [13] (Figs. 1–6). In this article, however, we used the segment tool in "paint on slices" for manual edition on the workstation, which can independently segment multiple regions, such as the liver, pancreas, and duodenum from the other abdominal lower attenuation (fat or air, etc.) on the same edited image. The adjustment of edited slab thickness each time can be controlled by the mouse scroll-wheel based on the dilated pancreatobiliary system. The whole edited slab thickness ranged 70–150 mm. After saving the image of 3D nCTCP with MinIP, a volume rendering mode was chosen to transfer the MinIP to VR image, and the duodenal image then could be segmented form pancreatobiliary system easily.

3.4. Tumor and liver outline

A tumor outline were grossly segmented from the surrounding structures also using the "paint on slices" segment tool, which based on a better discernible attenuation difference between tumor and surrounding structures from the late arterial or portal phase, For the hepatic morphologic outline, we chosen volume rendering mode during the portal phase and manually removed its surrounding structures from the liver volume. Tumor and liver morphologic outline is helpful in depicting the spatial relationship between intrahepatic or hilar lesions and the bile ducts and hepatic vasculatures (Figs. 1 and 5).

3.5. Multiphase fusion 3D images

All the postprocessed 3D images above were orderly saved in a "save/recall" file and each saved image could be recalled in a unique 3D VR display mode. Specifically, CTAG, CTPV, CTHV, and liver volume displayed using a "plateau" ramp in view of their hyperdense values; meanwhile, either nCTCP or duodenum using a "valley" ramp regarding their hypodense values. For the tumor morphologic display, either plateau or valley ramp was used based on its high or low attenuation values compared to enhanced hepatic or pancreatic parenchyma. In addition, "Smooth 3D+ " function was also adopted for further reducing the volume rendering image noise before fusion. After that, multiphase fusion images could be conducted according to the need of observed structures, but the maximal numbers of fused images from the "save/recall" file are seven objects on the present workstation. The transparency of each fused image can be adjusted through 1–100 % for optimization of object display (Figs. 1 and 5). Postprocessing time was approximately 10–15 min for 3D nCTCP, and 15 min for CTAG, CTPV, CTHV, and tumor and liver outline, respectively. A total of 25–30 min of extra postprocessing time was required to conduct the fusion images.

4. Discussion

Preoperative delineating of the spatial relationship between tumor morphology and adjacent structures is critical so that surgeons could be understood more easily before surgery in patients with malignant pancreatobiliary obstruction. Advanced postprocessing techniques of MDCT aid in the accurate assessment of the vascular anatomy and the presence and extent of tumor invasion into the hepatic artery, portal vein, and hepatic parenchyma [14]. Multiphase fusion images have the ability to depict the hepatic and peripancreatic arteries, portal and superior mesenteric veins, hepatic vein, pancreatobiliary system as well as liver, tumor and duodenal outline in one image. However, previous multiphase or multi-organ fusion image was also multi-procedure or multi-modality [5, 6, 15–17]. Therefore, high cost and longer work-up time for patients are inevitable. In this article, we introduced a novel method for multiphase fusion images, which was not published before.

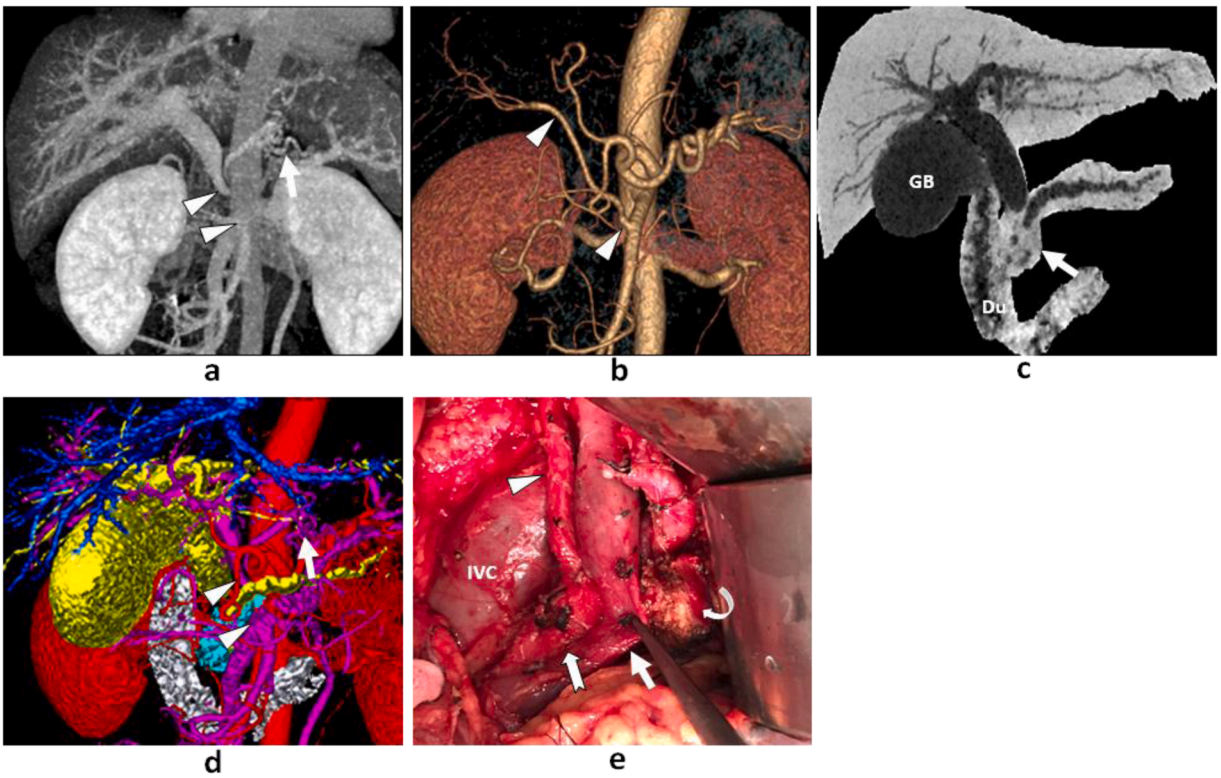

Fig. 3. A 49-year-old man with borderline resectable pancreatic head carcinoma. In this case, the portal vein occlusion of less than 2 cm segment at surgery was found because of tumor involvement but separable, in whom curative pancreatoduodenectomy was performed. Narrowing of the portal vein (arrowheads) with collaterals (arrow) on 3D CTPV with MIP (a) and the replaced right hepatic artery from the superior mesenteric artery (arrowheads) can be seen clearly on 3D CTAG with VR (b), respectively. Meanwhile, 3D nCTCP with MinIP (c) shows abrupt termination of both the common bile duct and pancreatic duct with a hypodense mass in the head of pancreas (arrow). Multiphase fusion images with VR (d) consisted of the pancreatobiliary system (yellow), main peripancreatic arteries (red), portal vein (purple), hepatic vein (blue), and duodenum (gray) show spatial relationship between tumor (green) and its surrounding structures, including the portal vein occlusion (arrowhead) and collaterals (arrow). Intraoperative photography (e) shows the replaced right hepatic artery (arrowheads) from the superior mesenteric artery (tailed arrow), separated portal vein (arrow) from tumor, and dissected pancreatic body (curved arrow). GB, gallbladder; Du, duodenum; IVC, inferior vena cava. (For interpretation of the references to color in this figure legend, the reader is referred to the web version of this article.)

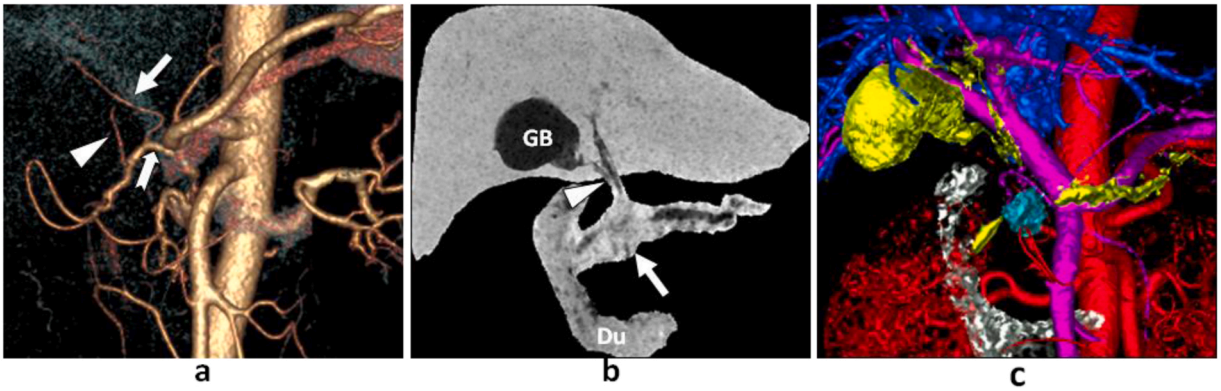

Fig. 4. A 57-year-old woman with pancreatic neck carcinoma underwent curative treatment. In this case, both the main peripancreatic arteries and vein were not tumor contact resulted in curative tumor resection. 3D CTGA with VR (a) shows accessory left (arrow) and right (arrowhead) hepatic arteries originated from the common hepatic artery (tailed arrow), and 3D nCTCP with MinIP (b) shows abrupt termination of both the common bile duct and pancreatic duct with a hypodense tumor in the neck of pancreas (arrow). Additionally, low insertion of the cystic duct (arrowhead) is also noted. Multiphase fusion images with VR (c) consisted of the pancreatobiliary system (yellow), main peripancreatic arteries (red), portal vein (purple), hepatic vein (blue), and duodenum (gray) show spatial relationship of tumor (green) to its adjacent structures. GB, gallbladder; Du, duodenum. (For interpretation of the references to color in this figure legend, the reader is referred to the web version of this article.)

With this method, enhanced dual-phase or multi-phase CT scan could be performed using intravenous contrast agent at one time, resulted in CTAG, CTPV, CTHV, and nCTCP generated concurrently. Accordingly, multiphase fusion images could be created without additional biliary contrast agent. Considering the application values of multiphase fusion imaging in surgery [5,6], we believe that one-stop evaluation of the regional anatomy between tumor and adjacent structures may be feasible with this technique.

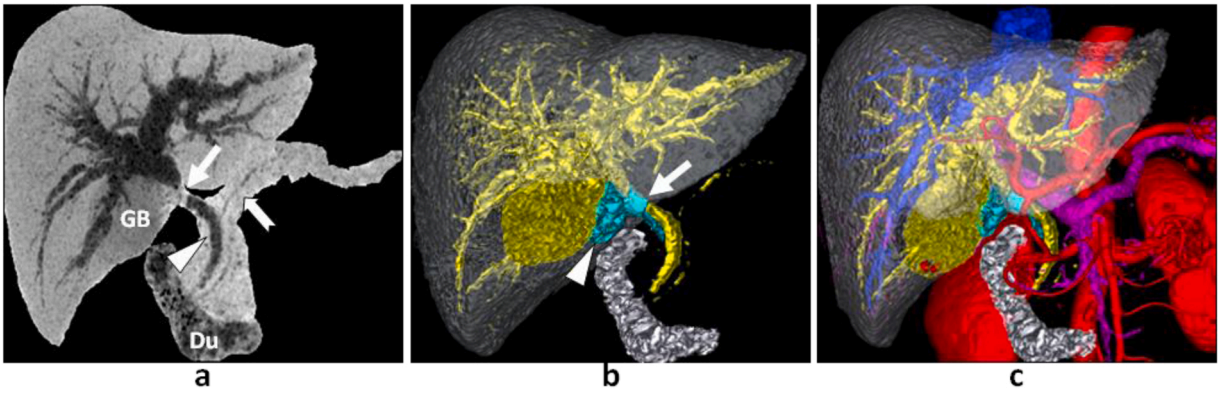

Fig. 5. A 69-year-old woman with gallbladder neck carcinoma resulted in I type perihilar obstruction according to Bismuth-Corlette classification [4] underwent curative treatment because of neither the main peripancreatic arteries nor veins involved by tumor, and cholecystectomy with choledochojejunostomy was performed. 3D nCTCP with MinIP (a) shows abrupt stricture on the common hepatic duct (arrow), but the distal common bile duct (arrowhead) and pancreatic duct (tailed arrow) are normal. Fused 3D nCTCP (yellow), tumor (green), duodenal (gray), and liver (30 % of transparency) images with VR (b) show spatial relations of gallbladder neck carcinoma (arrowhead) involved the common hepatic duct (arrow). Multiphase fusion images with VR (c) consisted of the pancreatobiliary system (yellow), main peripancreatic arteries (red), portal vein (purple), hepatic vein (blue), and duodenum (gray) entirely show anatomic relations of tumor (green) to main peripancreatic arteries and veins. GB, gallbladder; Du, duodenum. (For interpretation of the references to color in this figure legend, the reader is referred to the web version of this article.)

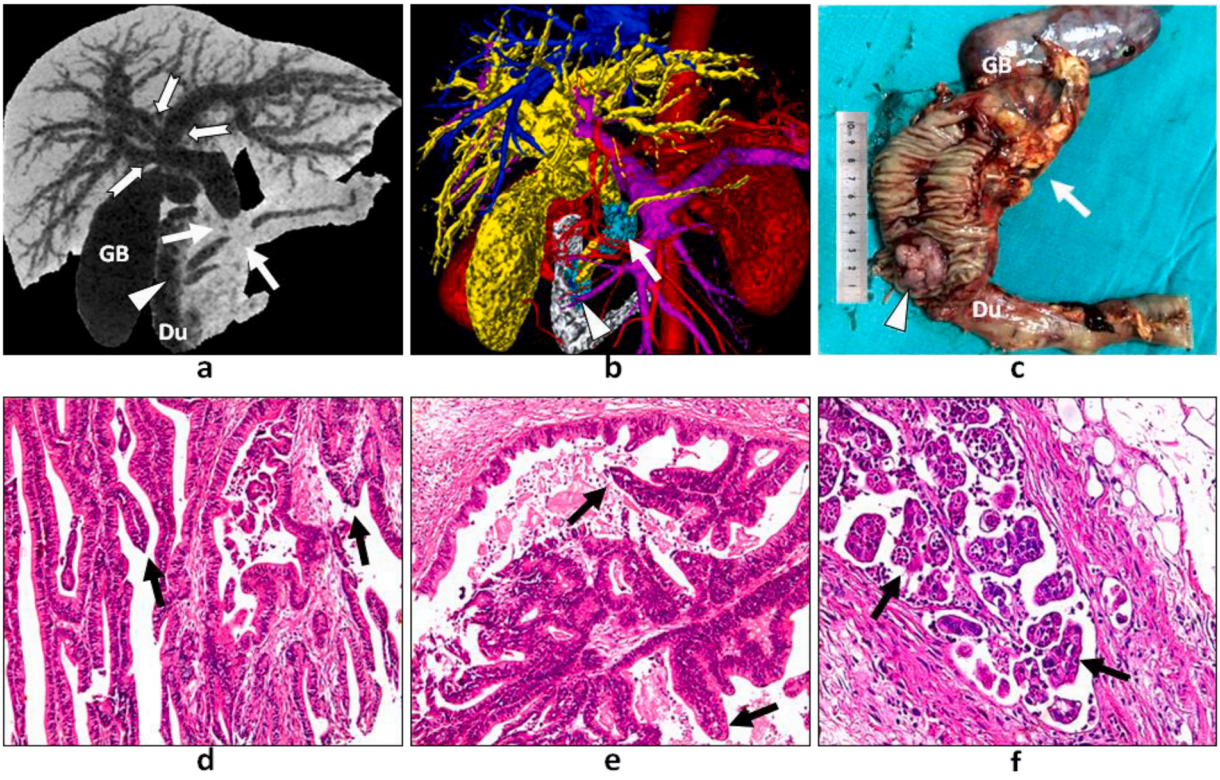

Fig. 6. A 68-year-old woman with ampullary adenocarcinoma and pancreatic head adenocarcinoma concomitantly who underwent curative treatment of pancreatoduodenectomy because there were no main peripancreatic vessels involvement. In this case, however, pancreatic head adenocarcinoma was postulated from ampullary adenocarcinoma. 3D nCTCP with MinIP (a) shows abrupt terminations of extrahepatic bile ducts and pancreatic ducts at locations of the pancreatic head (arrows) and ampulla of Vater (arrowhead), respectively. Meanwhile, trifurcation of biliary ducts also be showed (tailed arrows). Multiphase fusion images with VR (b) consisted of the pancreatobiliary system (yellow), main peripancreatic arteries (50 % of transparency, red), portal vein (purple), hepatic vein (blue), and duodenum (gray) show anatomic relations both of ampullary tumor (arrowhead, green) and pancreatic head tumor (arrow, green) to its surrounding structures. Macroscopically, tumors at the ampulla of Vater and pancreatic head (c) are observed concomitantly with size of 3.5 cm (arrowhead) and 4.0 cm (arrow), respectively. Histologic section of ampullary tumor (d) demonstrates multiple papillary structures (arrows) with adenocarcinoma cells (H&E, 100 ×). Histologic section of pancreatic head tumor (e) also demonstrates multiple papillary structures (arrows) with adenocarcinoma cells same as ampullary tumor, which are different from primary pancreatic adenocarcinoma (H&E, 100 ×). Microscopically, adenocarcinoma cells can be seen in lymphatic vessels (arrows, f) (H&E, 100 ×), thus, pancreatic head adenocarcinoma was postulated from ampullary adenocarcinoma. GB, gallbladder; Du, duodenum.(For interpretation of the references to color in this figure legend, the reader is referred to the web version of this article.)

Funding

This study was funded by "Wuxi Taihu Lake Talent Plan, Leading Talents in Medical and Health Profession".

Ethical statement

This study meets the requirements of the Declaration of Helsinki.

Conflict of interest

All authors declares that they have not an actual or potential conflict of interest including any financial, personal or other relationships with other people or organization, that can inappropriately influence the work.

References

[1] B.S. Kapoor, G. Mauri, J.M. Lorenz, Management of biliary strictures: state-of-the-art review, Radiology 289 (3) (2018) 590–603, https://doi.org/10.1148/radiol.2018172424.

[2] A. Singh, A. Gelrud, B. Agarwa, Biliary strictures: diagnostic considerations and approach, Gastroenterol. Rep. 3 (1) (2015) 22–31, https://doi.org/10.1093/gastro/gou072.

[3] I. Ryoo, J.M. Lee, H.S. Park, J.K. Han, B.I. Choi, Preoperative assessment of longitudinal extent of bile duct cancers using MDCT with multiplanar reconstruction and minimum intensity projections: comparison with MR cholangiography, Eur. J. Radiol. 81 (9) (2012) 2020–2026, https://doi.org/10.1016/j.ejrad.2011.06.007.

[4] X.P. Wu, J.M. Ni, Z.Y. Zhang, F.Q. Lu, B. Li, H.H. Jin, T. Dai, Preoperative evaluation of malignant perihilar biliary obstruction: negative-contrast CT cholangiopancreatography and CT angiography versus MRCP and MR angiography, Am. J. Roentgenol. 205 (4) (2015) 780–788, https://doi.org/10.2214/AJR.14.13983.

[5] M. Uchida, M. Ishibashi, N. Tomita, M. Shinagawa, N. Hayabuchi, K. Okuda, Hilar and suprapancreatic cholangiocarcinoma: value of 3D angiography and multiphase fusion Images using MDCT, Am. J. Roentgenol. 184 (5) (2005) 1572–1577, https://doi.org/10.2214/ajr.184.5.01841572.

[6] Y. Okuda, K. Taura, S. Seo, K. Yasuchika, T. Nitta, K. Ogawa, E. Hatano, S. Uemoto, Usefulness of operative planning based on 3-dimensional CT cholangiography for biliary malignancies, Surgery 158 (5) (2015) 1261–1271, https://doi.org/10.1016/j.surg.2015.04.021.

[7] E.P. Tamm, A. Balachandran, P. Bhosale, J. Szklaruk, Update on 3D and multiplanar MDCT in the assessment of biliary and pancreatic pathology, Abdom. Imaging 34 (1) (2009) 64–74, https://doi.org/10.1007/s00261-008-9416-4.

[8] M. Uchida, M. Ishibashi, J. Sakoda, S. Azuma, S. Nagata, N. Hayabuchi, CT image fusion for 3D depiction of anatomic abnormalities of the hepatic hilum, Am. J. Roentgenol. 189 (4) (2007) W184–W191, https://doi.org/10.2214/AJR.07.2280.

[9] M.M. Al-Hawary, I.R. Francis, S.T. Chari, E.K. Fishman, D.M. Hough, D.S. Lu, M. Macari, A.J. Megibow, F.H. Miller, K.J. Mortele, N.B. Mechant, R.M. Minter, E. P. Tamm, D.V. Sahani, D.M. Simeone, Pancreatic ductal adenocarcinoma radiology reporting template: consensus statement of the Society of Abdominal Radiology and the American Pancreatic Association, Gastroenterology 146 (1) (2014) 291–304.e1, https://doi.org/10.1053/j.gastro.2013.11.004.

[10] M.A. Tempero, M.P. Malafa, M. Al-Hawary, H. Asbun, A. Bain, S.W. Behrman, A. B. Benson III, E. Binder, D.B. Cardin, C. Cha, E.G. Chiorean, V. Chung, B. Czito, M. Dillhoff, E. Dotan, C.R. Ferrone, J. Hardacre, W.G. Hawkins, J. Herman, A. H. Ko, S. Komanduri, A. Koong, N. LoConte, A.M. Lowy, C. Moravek, E. K. Nakakura, E.M. O'Reilly, J. Obando, S. Reddy, C. Scaife, S. Thayer, C.D. Weekes, R.A. Wolff, B.M. Wolpin, J. Burns, S. Darlow, Pancreatic adenocarcinoma, version 2.2017, NCCN Clinical Practice Guidelines in Oncology, J. Natl. Compr. Cancer Netw. 15 (8) (2017) 1028–1061, https://doi.org/10.6004/jnccn.2017.0131.

[11] F.M. Chen, J.M. Ni, Z.Y. Zhang, L. Zhang, B. Li, C.J. Jiang, Presurgical evaluation of pancreatic cancer: a comprehensive imaging comparison of CT versus MRI, Am. J. Roentgenol. 206 (3) (2016) 526–535, https://doi.org/10.2214/AJR.15.15236.

[12] T. Denecke, E. Degutyte, L. Stelter, L. Lehmkuhl, R. Valencia, E. Lopez-Hänninen, R. Felix, C. Stroszczynski, Minimum intensity projections of the biliary system using 16-channel multidetector computed tomography in patients with biliary obstruction: comparison with MRCP, Eur. Radiol. 16 (8) (2006) 1719–1726, https://doi.org/10.1007/s00330-006-0172-y.

[13] B. Li, L. Zhang, Z.Y. Zhang, J.M. Ni, F.Q. Lu, W.J. Wu, C.J. Jiang, Differentiation of noncalculous periampullary obstruction: comparison of CT with negative-contrast CT cholangiopancreatography versus MRI with MR cholangiopancreatography, Eur. Radiol. 25 (2) (2015) 391–401, https://doi.org/10.1007/s00330-014-3430-4.

[14] I. Joo, J.M. Lee, J.H. Yoon, Imaging Diagnosis of intrahepatic and perihilar cholangiocarcinoma: recent advances and challenges, Radiology 288 (1) (2018) 7–13, https://doi.org/10.1148/radiol.2018171187.

[15] K. Ibukuro, T. Takeguchi, H. Fukuda, H. Fukuda, S. Abe, K. Tobe, R. Tanaka, K. Tagawa, Spatial relationship between intrahepatic artery and portal vein based on the fusion image of CT-arterial portography (CTAP) and CT-angiography (CTA): new classification for hepatic artery at hepatic hilum and the segmentation of right anterior section of the liver, Eur. J. Radiol. 81 (2) (2012) e158–e165, https://doi.org/10.1016/j.ejrad.2011.01.045.

[16] Y. Oshiro, R. Sasaki, K. Nasu, N. Ohkohchi, A novel preoperative fusion analysis using three-dimensional MDCT combined with three-dimensional MRI for patients with hilar cholangiocarcinoma, Clin. Imaging 37 (4) (2013) 772–774, https://doi.org/10.1016/j.clinimag.2013.02.002.

[17] R. Dorrell, S. Pawa, Y. Zhou, N. Lalwani, R. Pawa, The diagnostic dilemma of malignant biliary strictures, Diagnostics 10 (5) (2020) 337–351, https://doi.org/10.3390/diagnostics10050337.